Insulin-like growth factor-I receptor blockade by a specific tyrosine kinase inhibitor for human gastrointestinal carcinomas

Wenhua Piao,[1] Yu Wang,[1] Yasushi Adachi,[1] Hiroyuki Yamamoto,[1] Rong Li,[1] Arisa Imsumran,[1] Hua Li,[1] Tadateru Maehata,[1] Masanori Ii,[1] Yoshiaki Arimura,[1] Choon-Taek Lee,[2] Yasuhisa Shinomura,[1] David P. Carbone,[3] and Kohzoh Imai[1]

[1]First Department of Internal Medicine, Sapporo Medical University, Sapporo, Japan; [2]Division of Pulmonary and Critical Care Medicine, Department of Internal Medicine and Lung Institute, Seoul National University College of Medicine, Seoul, Korea; and [3]Vanderbilt-Ingram Cancer Center and Departments of Medicine and Cell Biology, Vanderbilt University, Nashville, Tenessee

Abstract

Insulin-like growth factor-I receptor (IGF-IR) signaling is required for carcinogenicity and proliferation of gastrointestinal (GI) cancers. In this study, we sought to evaluate the effect of a new tyrosine kinase inhibitor of IGF-IR, NVP-AEW541, on the signal transduction and the progression of GI carcinomas. We assessed the effect of NVP-AEW541 on signal transduction, proliferation, survival, and migration in four GI cancer cells: colorectal adenocarcinoma HT29, pancreatic adenocarcinoma BxPC3, esophageal squamous cell carcinoma TE1, and hepatoma PLC/PRF/5. The effects of NVP-AEW541 alone and with chemotherapy were studied *in vitro* and in nude mouse xenografts. We also analyzed the effects of NVP-AEW541 on insulin signals and hybrid receptor formation between IGF-IR and insulin receptor. NVP-AEW541 blocked autophosphorylation of IGF-IR and both Akt and extracellular signal-regulated kinase activation by IGF but not by insulin. NVP-AEW541 suppressed proliferation and tumorigenicity *in vitro* in a dose-dependent manner in all cell lines. The drug inhibited tumor as a single agent and, when combined with stressors, up-regulated apoptosis in a dose-dependent fashion and inhibited mobility. NVP-AEW541 augmented the effects of chemotherapy on *in vitro* growth and induction of apoptosis. Moreover, the combination of NVP-AEW541 and chemotherapy was highly effective against tumors in mice. This compound did not influence hybrid receptor formation. Thus, NVP-AEW541 may have significant therapeutic utility in human GI carcinomas both alone and in combination with chemotherapy. [Mol Cancer Ther 2008;7(6):1483–93]

Introduction

Signals from a variety of growth factors are required for tumorigenesis and cancer development in human malignancies (1), including gastrointestinal (GI) carcinomas (2). Tyrosine kinase receptors are one new group of targets and can be targeted by small-molecule tyrosine kinase inhibitors (TKI) or monoclonal antibodies. Insulin-like growth factor-I receptor (IGF-IR) signaling is able to potently stimulate tumor progression and cellular differentiation (3) and is a promising new molecular target in human malignancies (2, 4).

IGF-IR consists of two α and two β subunits in a heterotetramer (5). Binding of the ligands IGF-I and IGF-II to IGF-IR causes receptor autophosphorylation and activates multiple signaling pathways, including the mitogen-activated protein kinase/extracellular signal-regulated kinase (ERK) and phosphatidylinositide 3-kinase/Akt-1 pathways (6, 7). IGF-IR pathway activation is also regulated by IGF-binding proteins and IGF-II receptor (8–10).

Dysregulation of the IGF-I system has been implicated in the proliferation of numerous neoplasms (2, 11). Elevation of serum IGF-I increases the risk of developing several cancers, including colon (9), and IGF-IR is also important for tumor maintenance (12, 13). Blocking IGF-IR has been shown to induce apoptosis in tumors but produce only growth arrest in untransformed cells (1), implying that receptor blockade may have a greater therapeutic index than other strategies targeting fundamental cell mechanisms such as DNA synthesis or the cell cycle. The fact that IGF-IR knockout mice are viable indicates that relatively normal tissue development and differentiation occurs in the absence IGF-IR signaling (14).

IGF stimulate the proliferation of GI cancer cells, including colon, esophagus, hepatocellular, and pancreas, and blocking of IGF-IR signaling inhibits tumor growth (8, 15–22). Soluble IGF-II receptor rescues Apc(Min/+) intestinal adenoma progression induced by loss of IGF-II imprinting (10). Intestinal fibroblast-derived IGF-II has

Received 12/13/07; revised 4/2/08; accepted 4/9/08.

Grant support: Ministry of Education, Culture, Sports, Science, and Technology and Ministry of Health, Labour and Welfare, Japan, grants-in-aid and Vanderbilt SPORE in Lung Cancer grant CA90949.

The costs of publication of this article were defrayed in part by the payment of page charges. This article must therefore be hereby marked *advertisement* in accordance with 18 U.S.C. Section 1734 solely to indicate this fact.

Note: W. Piao, Y. Wang, and Y. Adachi contributed equally to this work.

Requests for reprints: Yasushi Adachi, First Department of Internal Medicine, Sapporo Medical University, S-1, W-16, Chuo-ku, Sapporo 060-8543, Japan. Phone: 81-11-611-2111, ext. 3211; Fax: 81-11-611-2282. E-mail: yadachi@sapmed.ac.jp

doi:10.1158/1535-7163.MCT-07-2395

been shown to stimulate proliferation of intestinal epithelial cells (23). Expression of both IGF-II and IGF-IR are increased in GI cancers (16, 18, 24, 25). IGF-I also has been shown to antagonize the antiproliferative effects of cyclooxygenase-2 inhibitors (26). IGF-IR signaling is also important in tumor dissemination through the control of adhesion, migration, and metastasis. These findings suggest a potential basis for tumor selectivity in therapeutic applications in GI cancers.

The insulin receptor (IR) is also a key component of the IGF signaling pathway. IR activation leads cell proliferation in addition to glucose metabolism. In addition to insulin, IR can also bind IGF-II and initiate mitogenic signaling (27). Two isoforms of IR are generated by alternative splicing of exon 11, A and B isoforms (28). IGF-IR and IR can form hybrid receptors that bind IGF at physiologic concentrations. IR and IGF-IR/IR hybrid receptors may also be involved in cancer biology as both insulin and IGF-I contribute to the development and progression of adenomatous polyps (29).

Several possible approaches to blocking IGF-IR signaling have been reported. Humanized monoclonal antibodies for IGF-IR are available (30–32) and some are in phase I trials. TKI for IGF-IR have been developed, including NVP-ADW742 (33), BMS-536924 (34), and BMS-554417 (dual targeting for IR and IGF-IR; ref. 35). We have constructed two dominant-negative inhibitors for IGF-IR (IGF-IR/dn), which are active as plasmids and recombinant adenovirus vectors in GI malignancies (18, 36–38).

The orally available compound NVP-AEW541, a pyrrolo[2,3-*d*]pyrimidine derivative, is a novel TKI for IGF-IR (39). It is highly selective against IGF-IR compared with other tyrosine kinases. There are only two reports about the effects of AEW541 on GI malignancies, hepatoma and neuroendocrine tumors (40, 41). As GI cancers are heterogeneous diseases, we analyzed the efficacy of this compound in esophageal squamous cell carcinoma, colorectal and pancreatic adenocarcinoma, and hepatoma. In this study, we assessed the effect of this TKI on signaling blockade, growth, apoptosis induction, migration, and *in vivo* therapeutic efficacy in s.c. xenografts. We also analyzed effects of this drug on insulin signaling and hybrid receptor formation. These observations strengthen the rationale for using NVP-AEW541 alone or in combination with chemotherapy in the molecular targeted therapy of GI cancers.

Materials and Methods

Materials, Cell Lines, and Mice

Anti-Akt-1 (c-20), anti-ERK1 (K-23), anti-phosphorylated ERK1 (E-4), ant-IGF-I (G-17), anti-IGF-IRα (2C8), and anti-IGF-IRβ (C20) were purchased from Santa Cruz Biotechnology and anti-phosphorylated Akt (Ser^{473}), anti-phosphorylated p44/42 mitogen-activated protein kinase (Thy^{202}/Tyr^{204}), and PathScan Multiplex Western Cocktail-I were from Cell Signaling Technology. Cisplatin and 5-fluorouracil (5-FU) were purchased from Sigma. Recombinant human IGF-I and IGF-II were purchased from R&D Systems. All human GI cancer cell lines were obtained from Japanese Cancer Collection of Research Bioresources Cell Bank. Cells were passaged in RPMI 1640 and DMEM with 10% fetal bovine serum. Specific pathogen-free female BALB/cAnNCrj-nu mice, 6 weeks old, were purchased from Charles River. The care and use of mice were according to our university' guidelines.

NVP-AEW541 was kindly provided by Novartis Pharma. Stock solution of this drug was prepared in DMSO and stored at −20°C.

Western Blotting and Immunoprecipitation

Cells were treated with 20 ng/mL IGF-I, 40 ng/mL IGF-II, or 10 nmol/L insulin as indicated in the text. Cell lysates were prepared as described previously (36). Equal aliquots of lysates (100 μg) were separated by 4% to 20% SDS-PAGE and immunoblotted onto polyvinylidene Hybond-P membrane (Amersham). Analysis was done using indicated antibodies, and bands were visualized by enhanced chemiluminescence (Amersham).

To analyze IGF-IR or IR signaling, 1 mg cell lysates were immunoprecipitated overnight at 4°C with anti-IGF-IR or anti-IR antibodies followed by Western blotting.

In vitro Cell Growth

Four thousand cells were seeded into a 96-well plate and each was treated with several concentrations of AEW541. Cell growth was measured using WST-1 reagent (Roche) as described previously (18).

Colony-Forming Activity

Cells (3×10^3 per plate) were seeded onto 60-mm culture plates and incubated for 24 h. The cells were then treated with NVP-AEW541 and were incubated for 14 days. After air drying, cells were fixed with methanol and stained with Giemsa solution. Colonies containing ≥50 cells were counted.

Assessment for Apoptosis

Caspase-3 colorimetric protease assay was done following the manufacturer's protocol (MBL). In brief, the caspase-3 activity of lysates (100 μg) was measured by colorimetric reaction at 400 nm. Early apoptosis were quantified by staining with Annexin V-FITC according to the manufacturer's protocol (BD Biosciences) and measured by flow cytometry. Terminal deoxynucleotidyl transferase–mediated dUTP nick end labeling assays were done with *in situ* apoptosis detection kit (Takara) following the manufacturer's protocol.

In vivo Therapeutic Efficacy in Established Tumors

HT29 cells (1×10^6) were s.c. injected into nude mice. After tumors were palpable (on day 24), animals were treated p.o. twice daily for 2 weeks either with NVP-AEW541 (40 mg/kg) or control. Three days after treatment, tumors were collected for analysis. Tumor diameters were serially measured with calipers and tumor volume was calculated using the formula: tumor volume (mm^3) = ($width^2 \times length$) / 2.

After HT29 tumors were palpable, animals were treated p.o. twice daily for 2 weeks with either NVP-AEW541 (40 mg/kg) or control. Both groups were then divided into

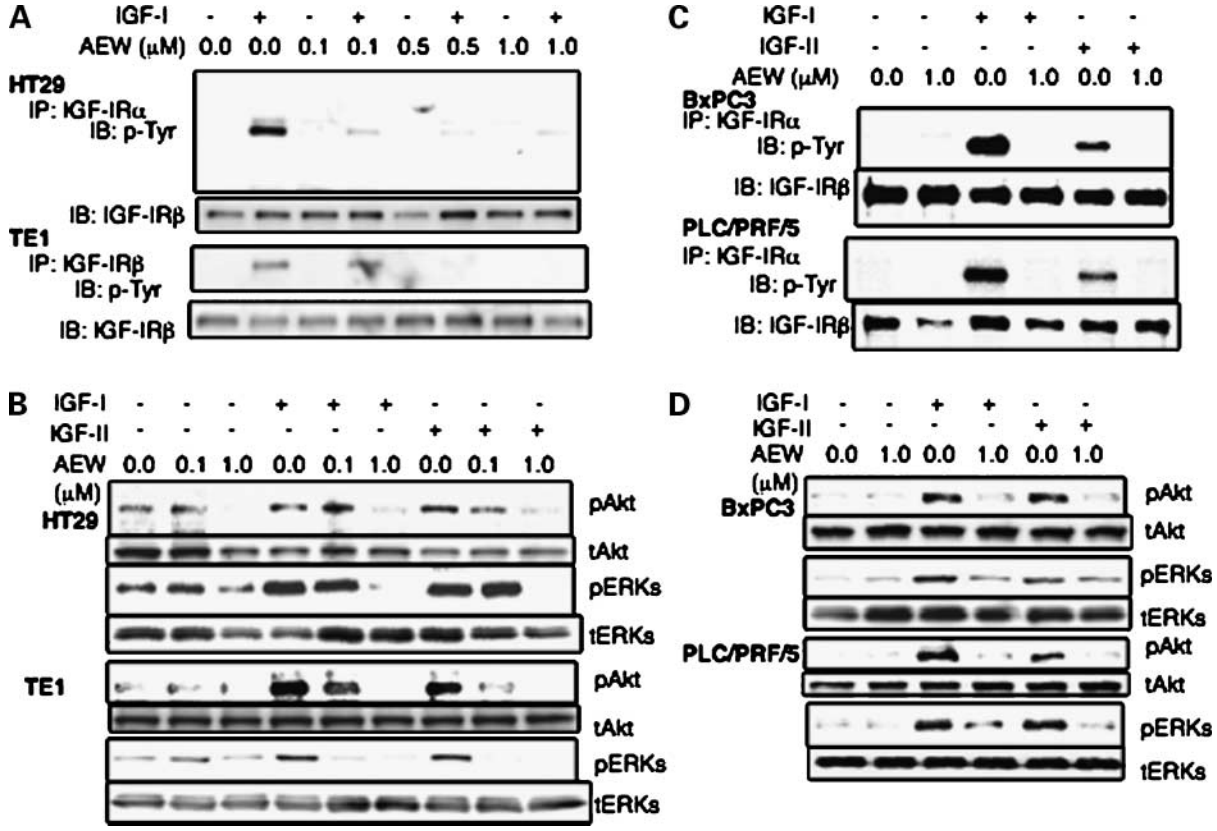

Figure 1. NVP-AEW541 blocked IGF/IGF-IR signals of GI cancer cell lines: colorectal adenocarcinoma HT29 (**A** and **B**), esophageal squamous cell carcinoma TE1 (**A** and **B**), pancreatic adenocarcinoma BxPC3 (**C** and **D**), and hepatocellular carcinoma PLC/PRF/5 (**C** and **D**). **A,** AEW541 reduced 20 ng/mL IGF-I-induced autophosphorylation of IGF-IR of HT29 and TE1 dose-dependently. **B,** AEW541 reduced both phosphorylation of Akt and ERK induced by both IGF-I and IGF-II with dose dependency in both HT29 and TE1. **C** and **D,** in both BxPC3 and PLC/PRF/5 cells, NVP-AEW541 blocked IGF-induced IGF-IR autophosphorylation (**C**) and its downstream phosphorylation of Akt and mitogen-activated protein kinases (**D**). *pTyr,* phosphorylated tyrosine; *pAkt,* phosphorylated Akt-1; *tAkt,* total Akt-1; *pERK,* phosphorylated ERK1/2; *tERK,* total ERK1/2.

pair-matched 5-FU-treated and control groups (administered i.p. once weekly for four doses). Mice were euthanized when tumors reached 2 cm in size or they developed clinically evident symptoms.

Immunohistochemical Analysis

Sections (5 μm) from formalin-fixed, paraffin-embedded tumor xenografts were prepared. After removed paraffin, the sections were pretreated with DakoCytomation Target Retrieval Solution (Dako) in a microwave (10 min). Then, endogenous peroxidase activity was blocked. Antibodies were applied after blocking with normal goat serum. Sections were incubated with the anti-rabbit secondary antibody (Santa Cruz Biotechnology) and a streptavidin-horseradish peroxidase (Dako) followed by exposure to the diaminobenzidine tetrahydrochloride substrate (Dako).

Measurement of immunostained area in pictures was done using the public domain NIH Image program.[4]

ELISA

Tumor samples were homogenized in Western blot lysis buffer and protein content was measured. Concentrations of IGF-IR, IR, and IGF were measured using the following ELISA kits according to the manufacturer's protocols: human IGF-I DuoSet, human total insulin R Duoset IC, and human total IGF-IR DuoSet IC (R&D Systems) and Active IGF-II ELISA Kit (Diagnostic Systems Laboratories).

Migration Assay

Wounding assays were done using a modification of the procedure described previously (18). Briefly, six-well chambers were prepared by scratching registration marks onto the slide surface. Cells were plated, grown normally for 48 h, and starved overnight. Cells were cut with a cell scraper and five images were captured 24 h later on an Olympus IX 71S1F-2 microscope using a ×20 objective. For each experiment, two independent observers counted the number of migrating cells.

Statistical Analysis

The results are presented as mean ± SE for each sample. The statistical significance of differences was determined by Student's two-tailed *t* test in two groups and done by

[4] Developed at the NIH and available on the Internet at http://rsb.info.nih.gov/nih-image/.

one-way ANOVA in multiple groups and two-factor factorial ANOVA. Survival curves were constructed according to the method of Kaplan-Meier. P values < 0.05 were considered to indicate statistical significance.

Results

Blockade of Signal Transduction

To investigate the effect of NVP-AEW541 on the IGF/receptor axis, we examined four GI cancer cell lines: HT29, TE1, BxPC3, and PLC/PRF/5. First, we evaluated NVP-AEW541 activity in HT29 by immunoprecipitation with anti-IGF-IRα and immunoblotting for phosphorylated tyrosine and IGF-IRβ. NVP-AEW541 reduced IGF-I-induced phosphorylation of IGF-IR in a dose-dependent manner and 1.0 μmol/L NVP-AEW541 blocked it completely (Fig. 1A). Then, we assessed the downstream signaling pathways of IGF-IR. This TKI blocked phosphorylation of Akt-1 and ERK both basal and that induced by both ligands in a dose-dependent manner (Fig. 1B).

Similarly, in TE1 cells, NVP-AEW541 reduced ligand-induced IGF-IR autophosphorylation and phosphorylation of Akt-1 and ERK in a dose-dependent manner (Fig. 1A and B). In BxPC3 and PLC/PRF/5 cells, 1 μmol/L NVP-AEW541 also reduced the ligand-induced phosphorylation of IGF-IR and its downstream signal activity (Fig. 1C and D). Thus, AEW541 effectively interrupted phosphorylation of IGF-IR and its downstream signals in GI cancers.

Reduction of Cell Growth *In vitro*

NVP-AEW541 reduced the growth on plastic of all GI cancer cells in a dose-dependent manner as analyzed by the WST-1 assay (Fig. 2A). Moreover, AEW541 dramatically reduced the *in vitro* tumorigenicity of all cells dose-dependently as assessed by colony formation assay (Fig. 2B). These results indicate that NVP-AEW541 effectively blocks the carcinogenicity and proliferation of multiple GI cancers.

Suppression of Mobility

To assess the effects of NVP-AEW541 on migration of GI cancer cells, we did wounding assays. AEW541 suppressed migration of HT29 (Fig. 2C). The number of migrated cells treated is significantly reduced compared with control. The compound significantly inhibited motility of other cells. The results indicate that NVP-AEW541 may have potential prevention for metastasis and tumor progression.

Effect on Survival

NVP-AEW541 also dramatically increased terminal deoxynucleotidyl transferase–mediated dUTP nick end labeling–positive cells in GI cancers (Fig. 3A). These results were confirmed by Annexin V assay (Fig. 3B), NVP-AEW541 increased the percentage of cells in early apoptosis. In BxPC3 cells, apoptotic induction was observed in 0.5 μmol/L NVP-AEW541.

We assessed the effect of NVP-AEW541 on stressor-induced apoptosis. Caspase-3 assay revealed that serum starvation did not induce apoptosis in HT29 but did induce apoptosis in the presence of NVP-AEW541 (Fig. 3C). Heat-induced caspase-3 activity and NVP-AEW541 up-regulated heat shock–induced apoptosis in both HT29 and BxPC3 (Fig. 3C). This result was confirmed by Annexin V assay in HT29, BxPC3, and PLC/PRF/5 (Fig. 3D). In TE1, NVP-AEW541 increased the percentage of cells undergoing apoptosis in response to ethanol (Fig. 3D).

Combination Effects with Chemotherapy

The effects of NVP-AEW541 in combination with chemotherapy was assessed. Colony formation assays revealed that cisplatin reduced the number of colonies in a dose-dependent manner in all cells and NVP-AEW541 significantly enhanced the effect of cisplatin (Fig. 4A). Both cisplatin and 5-FU alone induced caspase-3 activity in all cells (Fig. 4B and C), and NVP-AEW541 significantly enhanced chemotherapy-induced apoptosis with all combinations, except for cisplatin in PLC/PRF/5 and 5-FU in TE1. These results suggest that IGF-IR may play critical roles in tumor progression and that NVP-AEW541 enhances the effects of chemotherapies.

NVP-AEW541 Suppressed Tumor on Mice

To assess the effect of this drug on *in vivo* GI cancer, HT29 cells were inoculated in nude mice and allowed to form evident tumors. Oral administration of 40 mg/kg NVP-AEW541 (twice daily for 2 weeks) significantly inhibited HT29 tumor growth on mice (Fig. 5A).

As this TKI up-regulated 5-FU-induced apoptosis *in vitro*, the effect of combined IGF-blockade with 5-FU on established tumors was then assessed. HT29 tumor-bearing mice were treated with NVP-AEW541 along with 5-FU or PBS. Although either 5-FU or NVP-AEW541 suppressed tumor growth, the combination therapy was much more effective than either treatment alone (Fig. 5B). These treatments did not have an adverse effect on the body weight of the treated mice, suggesting tolerable toxicity. This indicates that NVP-AEW541 has significant potential to enhance the effect of chemotherapy in GI cancers.

To evaluate the effect of AEW541 on IGF-IR downstream signals in tumors, immunohistochemical analysis (Fig. 5C) and ELISA (Fig. 5D) were done. Immunohistochemically positive areas were quantitatively measured using densitometry and NIH image software, and this revealed that AEW541 inhibited both activation of Akt and ERK (Fig. 5C) without influence on IGF-IR expression. This compound blocked phosphorylation of Akt-1 more than that of the ERK. HT29 did not express IGF-I by ELISA at all (data not shown), and AEW541 did not affect on the expression of IGF-II, IGF-IR, and IR (Fig. 5D) in HT29 tumors on mice. These data suggest that this TKI effectively blocks IGF-IR signals without affecting the expression of IGF-IR/IR pathway proteins.

Effect on Insulin Signals and Hybrid Receptor

As IGF-IR has homology with the IR, we assessed the effects of this inhibitor on insulin signaling. First, we assessed the expression of IR isoforms in GI cancer cells. All cells expressed both isoforms (Fig. 6A). Although both HT29 and BxPC3 express A isoform mainly, both PLC/PRF/5 and TE1 express both isoforms equally.

To define the effects of NVP-AEW541 on downstream signaling of IR in HT29, Western blotting was done.

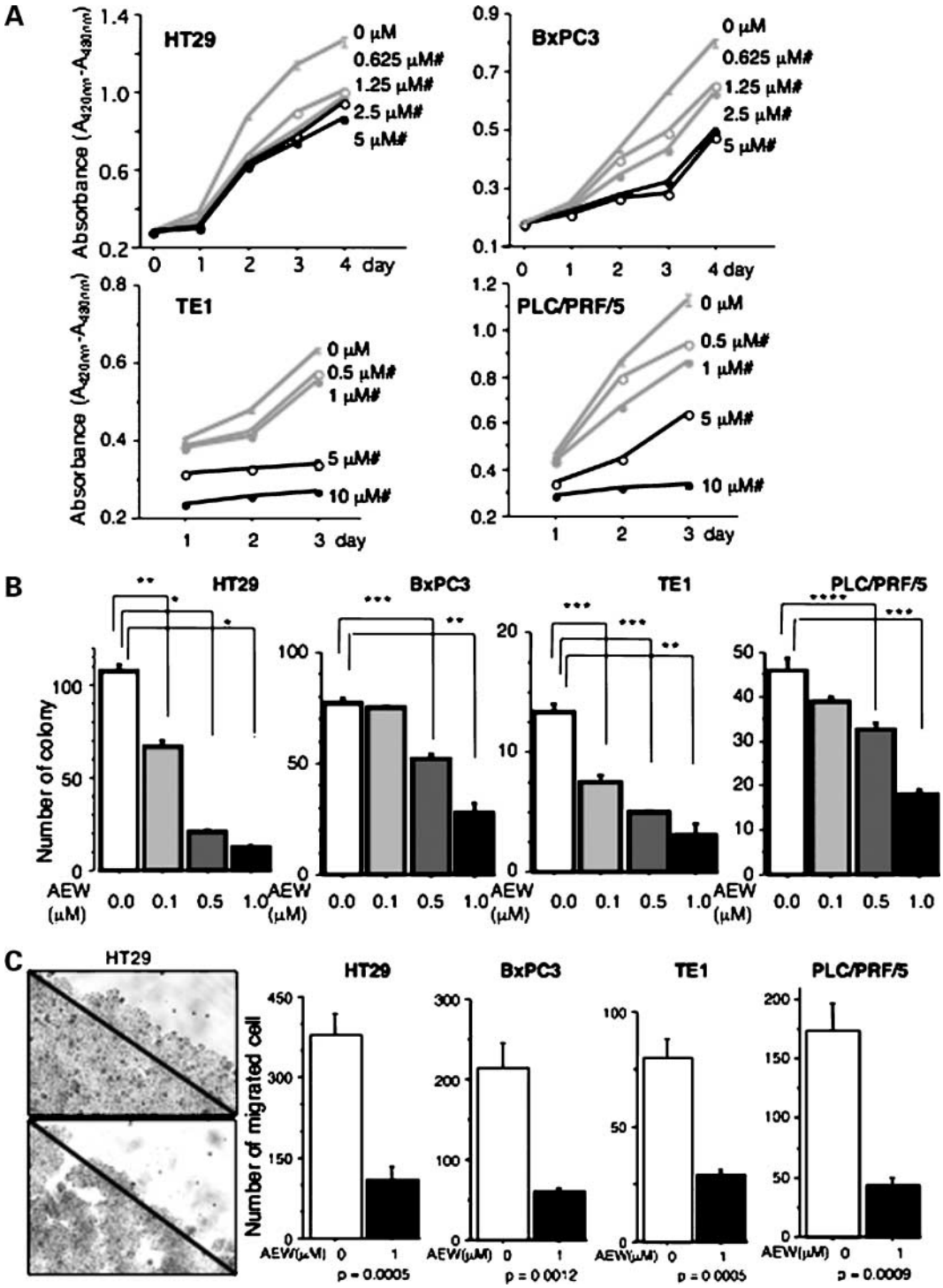

Figure 2. NVP-AEW541 reduces tumor growth and migration of GI cancer cell lines. **A,** starting 24 h after seeding, cancer cells were cultured in conditioned medium with different concentrations of NVP-AEW541 and cell growth was measured using the WST-1 assay. NVP-AEW541 reduced the growth of GI cancer cell lines on plastic in a dose-dependent manner. #, $P < 0.0001$ compared with the cells without AEW541. **B,** GI cancer cells were cultured 14 d with different concentrations of NVP-AEW541 as described in Materials and Methods. Colony formation assay shows that NVP-AEW541 reduces *in vitro* tumorigenicity of GI cancers in a dose-dependent manner. *, $P < 0.0001$; **, $P < 0.001$; ***, $P < 0.01$; ****, $P < 0.05$. **C,** migration assays were done as described in Materials and Methods. After the cell monolayer was cut with a cell scraper, AEW541 was added to the medium. Wounding assays shows that HT29 cells treated with control moved from scratched line to right and upper directions (*top left*); however, the TKI suppressed this mobility (*bottom left*). The summary of migration assay shows that AEW541 reduced the number of migrated cells significantly: HT29 ($P = 0.0005$), BxPC3 ($P = 0.0012$), TE1 ($P = 0.0005$), and PLC/PRF/5 ($P = 0.0009$).

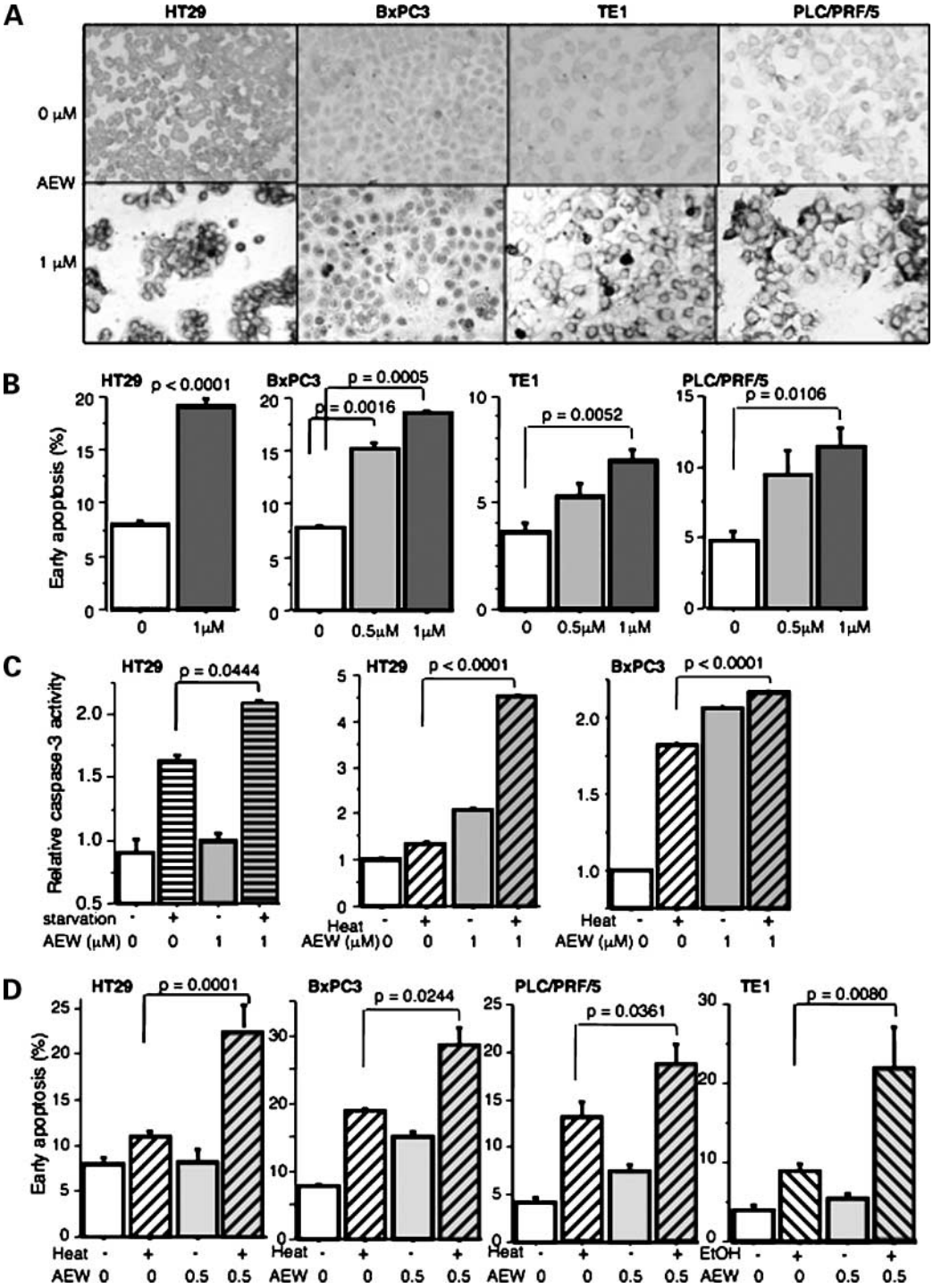

Figure 3. NVP-AEW541 induces apoptosis and up-regulates stressor-induced apoptosis in GI cancer cell lines. Twenty-four hours after seeding, cells were treated with NVP-AEW541. **A,** GI cancer cells were cultured in FCS-containing medium with or without 1 μmol/L NVP-AEW541 for 48 h and terminal deoxynucleotidyl transferase–mediated dUTP nick end labeling assays were done. NVP-AEW541 induced apoptosis in four GI cell lines. **B,** cells were cultured in FCS-containing medium and treated with different concentrations of NVP-AEW541 for 48 h. Annexin V assay reveals that NVP-AEW541 up-regulates early apoptosis dose-dependently in HT29 ($P < 0.0001$), BxPC3 ($P = 0.0016$ in 0.5 μmol/L AEW541 and $P = 0.0005$ in 1.0 μmol/L AEW541), TE1 ($P = 0.0052$), and PLC/PRF/5 ($P = 0.0106$). Cells undergoing (early) apoptosis showed an increase in Annexin V binding but excluded propidium iodide. **C,** caspase-3 assay shows that starvation-induced (24 h) and heat shock–induced (42°C for 30 min) apoptosis is up-regulated by treatment with 1 μmol/L NVP-AEW541 in HT29 (starvation, $P = 0.0444$; heat, $P < 0.0001$) and BxPC3 (heat, $P < 0.0001$). **D,** Annexin V assay reveals that 0.5 μmol/L NVP-AEW541 enhances heat-induced (42°C for 30 min) and 10% ethanol-induced (1 h) early apoptosis in four GI cells: HT29 ($P = 0.0001$), BxPC3 ($P = 0.0224$), PLC/PRF/5 ($P = 0.0361$), and TE1 ($P = 0.0080$).

Although insulin induces both phosphorylation of Akt and the ERK, the TKI did not block this phosphorylation (Fig. 6B). Immunoprecipitation with anti-IR followed by immunoblotting for phosphotyrosine or IR revealed that this inhibitor did not block insulin-induced phosphorylation of IR (Fig. 6B). The result is confirmed in TE1 (Fig. 6B). These data indicate that NVP-AEW541 can block IGF signaling without detectable effects on insulin signaling under these conditions.

We assessed heterodimerization of IGF-IR and IR in both HT29 and TE1. IGF-IR was detected in all samples immunoprecipitated with anti-IR (Fig. 6B), showing that NVP-AEW541 does not influence this heterodimerization. This was confirmed by the observation that IR was also identified in all immunoprecipitations with anti-IGF-IR, although AEW541 blocked IGF-induced phosphorylation of IGF-IR (Fig. 6C). In BxPC3 and PLC/PRF/5 (Fig. 6D), IGF-IR was detected equally in the presence or absence of this drug after immunoprecipitation with anti-IR. TKI also did not affect IR pull-down in cells immunoprecipitated with anti-IGF-IR. These results indicate that low dose of 1 μmol/L NVP-AEW541 selectively blocks IGF-IR signaling.

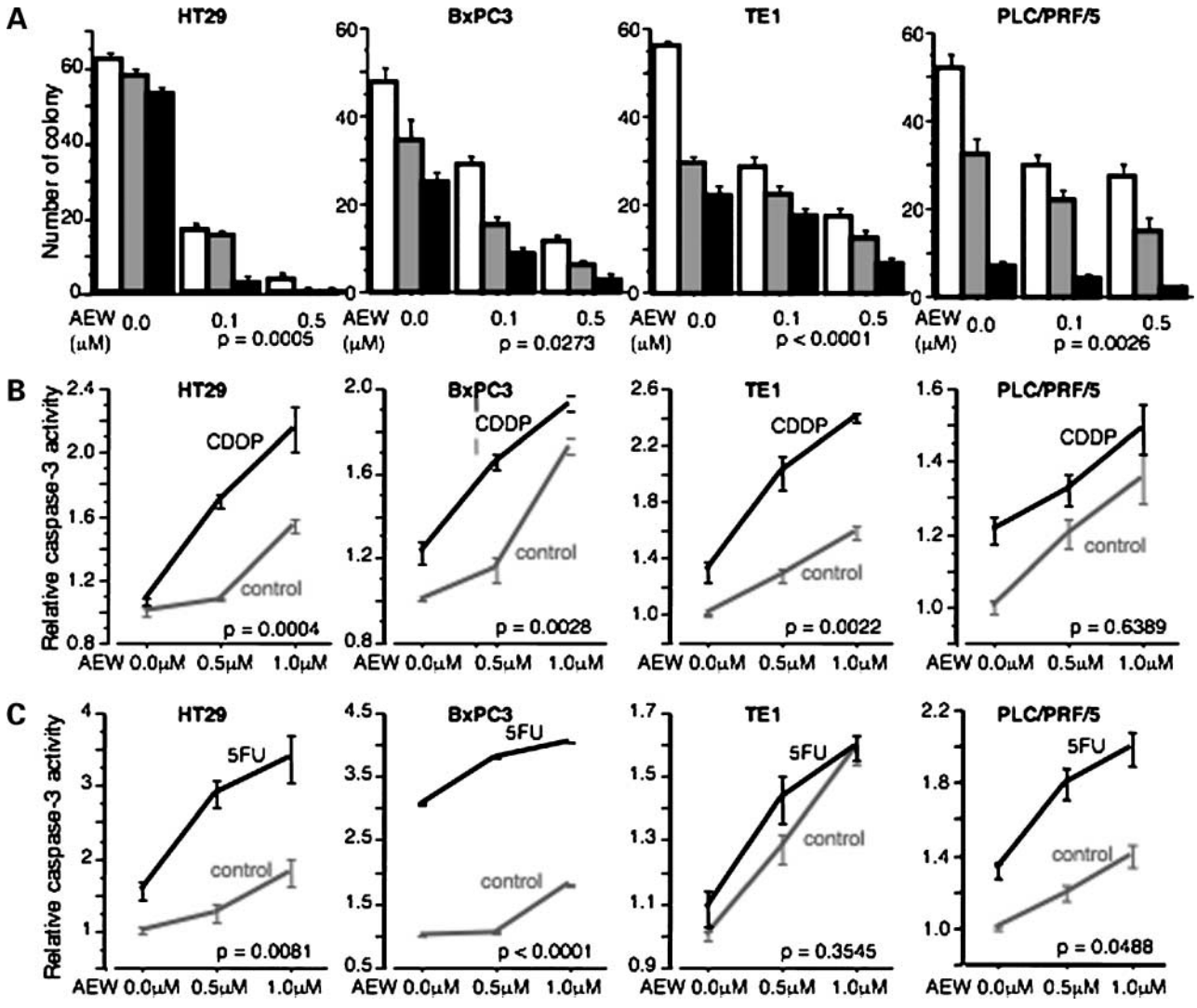

Figure 4. NVP-AEW541 strengthens chemotherapy. Twenty-four hours after seeding, cells were treated with NVP-AEW541 and cisplatin/5-FU. **A,** cells were cultured with combinations of the indicated different concentrations of cisplatin and three doses of AEW541 for 2 wk. Colony formation assay shows that NVP-AEW541 enhances significantly cisplatin-induced suppression of *in vitro* tumorigenicity of GI cancer cells: HT29 ($P = 0.0005$), BxPC3 ($P = 0.0273$), TE1 ($P < 0.0001$), and PLC/PRF/5 ($P = 0.0026$). *White column,* cells without cisplatin; *gray column,* cells treated with 10 μmol/L cisplatin; *black column,* cells treated with 50 μmol/L cisplatin. **B,** cells were treated with combinations of 50 μmol/L cisplatin and three different concentrations of AEW541 for 24 h, and apoptosis was assessed. Caspase-3 assay reveals that NVP-AEW541 up-regulates cisplatin-induced apoptosis in four GI cancer cells: HT29 ($P = 0.0004$), BxPC3 ($P = 0.0028$), TE1 ($P = 0.0022$), and PLC/PRF/5 ($P = 0.6389$). **C,** cells were cultured with combinations of 260 μmol/L 5-FU and three different concentrations of AEW541 for 24 h. Caspase-3 assay reveals that NVP-AEW541 up-regulates 5-FU-induced apoptosis in four GI cancer cells: HT29 ($P = 0.0081$), BxPC3 ($P < 0.0001$), TE1 ($P = 0.3545$), and PLC/PRF/5 ($P = 0.0488$). *Black line,* cells treated with cisplatin (**B**) or 5-FU (**C**); *gray line,* cells without chemotherapy.

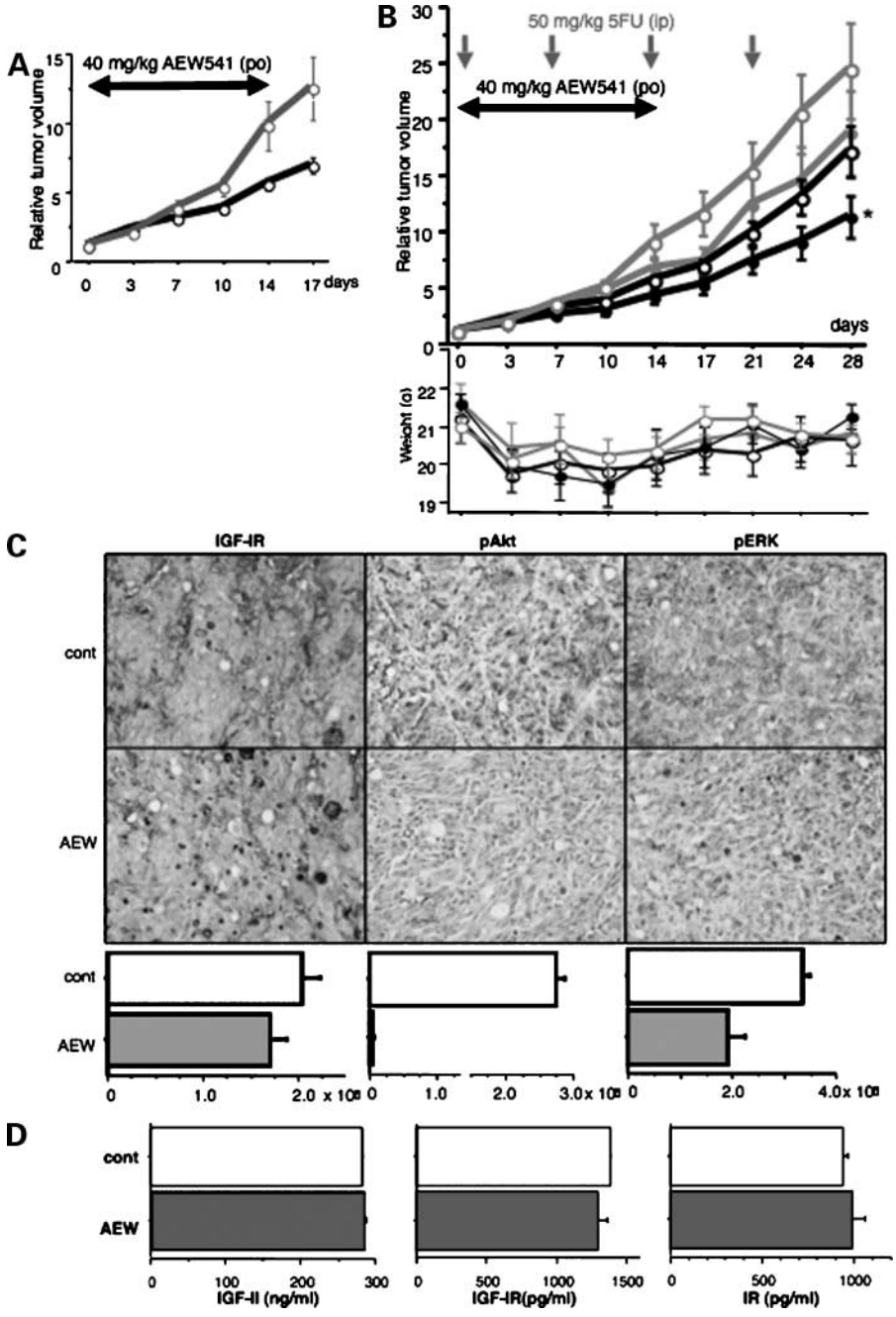

Figure 5. Effect of AEW541 on HT29 established s.c. tumors on nude mice. **A,** 1×10^6 HT29 cells were s.c. injected into 28 nude mice. After tumors were palpable (on day 24), animals were treated p.o. twice daily for 2 wk, 7 d weekly with either NVP-AEW541 (40 mg/kg; 10 mL/kg dissolved in 25 mmol/L L(+)-tartaric acid) or 25 mmol/L L(+)-tartaric acid (control). NVP-AEW541 reduces HT29 tumor growth on nude mice ($P < 0.05$, $n = 14$). *Gray open circle,* control; *black open circle,* NVP-AEW541. **B,** 1×10^6 HT29 were s.c. injected into 72 nude mice. After tumors were palpable, animals were treated p.o. twice daily for 2 wk, 7 d weekly with either NVP-AEW541 (40 mg/kg) or L(+)-tartaric acid. Both groups were then divided into pair-matched chemotherapy-treated and control groups ($n = 18$ per group). 5-FU (50 mg/kg) or vehicle was administered i.p. once weekly for four doses. AEW541 enhanced the tumor suppressive effect of 5-FU. Combination of NVP-AEW541 and 5-FU is most effective in suppression of tumor growth on nude mice. *, $P < 0.05$, compared with control ($n = 18$). There is no difference in mouse weight in each group. *Gray open circle,* control; *gray closed circle;* 5-FU alone; *black open circle,* NVP-AEW541 alone; *black closed circle,* combination of 5-FU and NVP-AEW541. **C,** anti-IGF-IR (c-20), anti-phosphorylated Akt (Ser^{473}), and anti-phosphorylated p44/42 mitogen-activated protein kinase (Thr^{202}/Tyr^{204}) were used for immunohistochemical analyses, and immunohistochemical-positive area was then quantitatively measured using NIH image software. The expression of total IGF-IR in the tumors treated with AEW541 is not different from that of control ($P = 0.2736$). Akt was much phosphorylated in tumors treated with control and AEW541 blocked clearly in those with the TKI ($P < 0.0001$). Although ERK were also phosphorylated in the control tumors, those phosphorylation were reduced by NPV-AEW541 ($P = 0.00193$). **D,** ELISA revealed that the expressions of IGF-II, IGF-IR, and IR in HT29 tumors on mice were not influenced by the treatment with NPV-AEW541 at all.

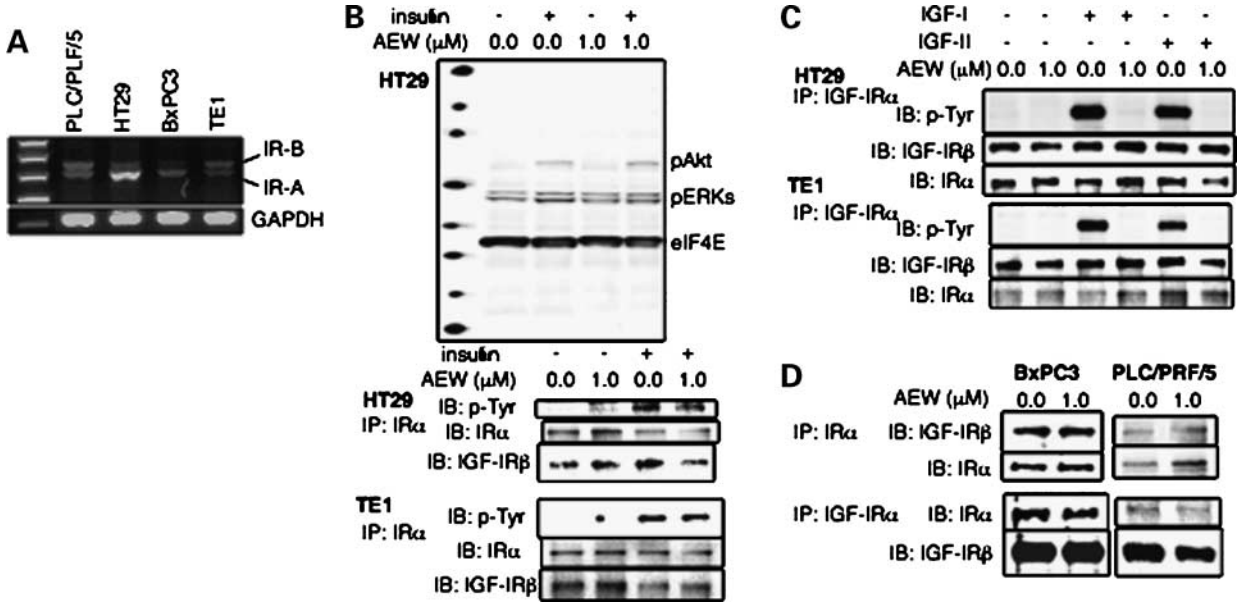

Figure 6. NVP-AEW541 does not effect on insulin signals and hybrid receptor formation with IGF-IR and IR of GI cancer cell lines. **A,** reverse transcription-PCR for IR isoforms was carried out as described previously using oligonucleotide primer sets for the amplification of IR cDNA sequences 5′-AACCAGAGTGAGTATGAGGAT-3′ and 5′-CCGTTCCAGAGCGAAGTGCTT-3′. PCR amplification was carried out for 30 cycles of 20 s at 96°C, 30 s at 58°C, and 1.5 min at 72°C (50). HT29 and BxPC3 express IR-A isoform mainly; however, PLC/PLF/5 and TE1 express both IR-A and IR-B isoforms. **B,** AEW541 did not affect 10 nmol/L insulin-induced phosphorylation of both Akt and ERK in HT29 immunoblotted by PathScan Multiplex Western Cocktail-I. Both HT29 and TE1 were cultured in serum-free medium with or without the TKI and then stimulated with insulin. Cell lysates were immunoprecipitated by anti-IRα and then immunoblotted for phosphotyrosine, IR, or IGF-IRβ. AEW541 did not reduce insulin-induced phosphorylation of IR. The drug did not alter the expression level of IR and dimer formation with IGF-IR. **C,** both HT29 and TE1 were cultured in serum-free medium with or without the TKI and then stimulated with IGF-I or IGF-II. Cell lysates were immunoprecipitated by anti-IGF-IRα and then immunoblotted for phosphotyrosine, IR, or IGF-IRβ. Although NVP-AEW541 blocked IGF-induced IGF-IR phosphorylation, AEW541 did not affect on heterodimerization of IGF-IR and IR. **D,** BxPC3 and PLC/PRF/5 were cultured with or without AEW541, and lysates were immunoprecipitated with anti-IRα or anti-IGF-IRα. NPV-AEW541 did not influence the hybrid receptor formation.

Discussion

GI cancers are frequently diagnosed in advanced stages with lymph node and distant metastases and peritoneal dissemination, and there is a paucity of meaningful treatment strategies for these tumors. IGF-mediated growth responsiveness is found in most GI cancer cells (15, 18, 19, 22). Aberrant activation of IGF-IR by paracrine and autocrine loops has been reported (22, 42), and the expression of IGF-IR/IGF-II may be useful for the prediction of recurrence and poor prognosis in esophageal squamous cell carcinoma (18). Here, we used a new IGF-IR-specific TKI, NPV-AEW541, for the accurate dissection of the responsible signaling pathways. Even in nanomolar concentrations, this agent suppressed colony formation efficiency and enhanced chemotherapy-induced apoptosis *in vitro* and chemotherapeutic efficacy *in vivo*. These results indicate that this strategy is promising for the treatment of GI cancers not only as a monotherapy but also to enhance the efficacy of chemotherapy. We show that AEW541 is effective against a wide range of GI carcinomas, with low toxicity in animal models. Blockade of phosphatidylinositide 3-kinase abrogates IGF-induced transmigration (43). As migration is one of critical steps for cancer progression, especially invasion and metastasis, it is worthwhile that NVP-AEW541 can inhibit the mobility of all four GI cancers studied.

A major hurdle to the targeting of IGF-IR is the close homology of the IGF-IR and the IR kinase domains. The ATP-binding site of these two receptors displays 100% sequence identity, whereas the entire kinase domains share 84% sequence identity, both with each other and across species (44). Therefore, it is very important that any strategy designed to block IGF-IR signaling has specificity for IGF-IR and without significant influence on IR signaling. We show here that AEW541 does not suppress insulin-induced IR or Akt phosphorylation, indicating a high degree of receptor selectivity at tumor-active doses with this molecular targeted therapy. Both receptors can form not only homodimers but also heterodimers. However, AEW541 does not influence this heterodimerization. Although high doses of AEW541 can block several tyrosine kinase receptors including IR, we show that concentrations of this compound active against GI cancers (≤1.0 μmol/L) inhibit IGF-IR signals selectively without affecting insulin signals. NVP-AEW541 shows a 27-fold inhibitory selectivity for the IGF-IR versus IR (39) and is slightly more active (IGF-IR kinase IC_{50}, 0.086 mol/L) and is more selective than another TKI, NVP-ADW742 (33, 45). Although plasma glucose and insulin were not monitored in mice treated with active doses of NVP-AEW541 to assess the potential risk of hypoglycemia, body weight was monitored and not

significantly affected by TKI therapy. These results confirm our biochemical findings. A recent article reported an initial weight loss, with a significant decrease of serum glucose due to increased glucose uptake at cellular level, in mice bearing Ewing's sarcoma, similar to the weight loss observed in mice treated with vincristine (46). The weight changes in our study are similar to their cohort of mice, which started to grow again after the first days of treatment. This lack of effect on the insulin pathway is very important for avoiding adverse effects in clinical applications. In addition, NVP-AEW541 has the advantage of being orally bioavailable.

However, some articles have recently reported several effects of IGF-IR blockade on IR. Both a chimeric single-chain antibody against IGF-IR (scFv-Fc) and a murine antibody for IGF-IR (EM164) resulted in decreased levels of IR *in vitro* and *in vivo* despite their lack of reactivity against IR (29). The down-regulation of IR by those anti-IGF-IR monoclonal antibodies requires the coexpression of IGF-IR and might be due to the endocytosis of hybrid IR/IGF-IR. IGF-IR down-regulation by small interfering RNA did not affect IR levels but, interestingly, did sensitize cells to insulin activation of downstream signaling pathways in breast cancer cells (47). IGF-IR small interfering RNA treatment diminished hybrid receptor formation, suggesting that specific down-regulation of IGF-IR resulted in enhanced holo-IR formation and insulin sensitivity. The expression IGF/IGF-IR and IR were not changed by this TKI, indicating that NVP-AEW541 might induce neither positive nor negative feedback in IGF-IR/IR axis in mice.

There are thus two opposing strategies for blockade IGF-IR signaling. One is to avoid adverse effects by shutting down only IGF-IR signaling without influencing IR signaling. Such selective IGF-IR blockade can be achieved by low-dose NVP-AEW541 or IGF-IR/dn for prevention of recurrence or maintenance of remission. Low dose of AEW541 shows clear antitumor effects not only by itself but also in combination with commonly used chemotherapy drugs. The other approach is to achieve maximum antitumor effects by blocking both IGF-IR and IR simultaneously using scFv-Fc, BMS-554417, or high-dose NVP-AEW541. This latter approach is likely to be significantly more toxic.

Recently, a new role for the IGF-IR has been identified with the demonstration that there is significant crosstalk between the IGF-R and other tyrosine kinase receptors. For example, many breast cancer patients who achieve an initial response to trastuzumab acquire resistance within 1 year from treatment initiation. One mechanism of resistance has been shown to be overexpression of IGF-IR (48) and another is the formation of IGF-IR/Her2 heterodimers in the resistant tumors (49). These data suggest that selective IGF-IR blockade may be specifically effective for breast cancer patients with trastuzumab resistant tumors.

Thus, in this study, we show that NVP-AEW541 suppresses tumorigenicity, survival, and migration by blocking Akt and ERK activation both *in vitro* and in animal models. It also potentiated chemotherapy efficacy without significantly influencing insulin signals at therapeutically effective doses. These studies thus validate IGF-IR as a therapeutic target in GI malignancies and suggest that NVP-AEW541 may be a promising anticancer therapeutic.

Disclosure of Potential Conflicts of Interest

No potential conflicts of interest were disclosed.

References

1. Baserga R. Oncogenes and the strategy of growth factors. Cell 1994; 79:927 – 30.

2. Adachi Y, Yamamoto H, Imsumran A, et al. Insulin-like growth factor-I receptor as a candidate for a novel molecular target in the gastrointestinal cancers. Dig Endosc 2006;18:245 – 51.

3. Sara VR, Hall K. Insulin-like growth factors and their binding proteins. Physiol Rev 1990;70:591 – 614.

4. Miller BS, Yee D. Type I insulin-like growth factor receptor as a therapeutic target in cancer. Cancer Res 2005;65:10123 – 7.

5. Ullrich A, Gray A, Tam AW, et al. Insulin-like growth factor I receptor primary structure: comparison with insulin receptor suggests structural determinants that define functional specificity. EMBO J 1986;5:2503 – 12.

6. Baselga J, Norton L, Albanell J, Kim YM, Mendelsohn J. Recombinant humanized anti-HER2 antibody (Herceptin) enhances the antitumor activity of paclitaxel and doxorubicin against HER2/*neu* overexpressing human breast cancer xenografts. Cancer Res 1998;58:2825 – 31.

7. Yu H, Rohan T. Role of the insulin-like growth factor family in cancer development and progression. J Natl Cancer Inst 2000;92:1472 – 89.

8. Remacle-Bonnet M, Garrouste F, el Atiq F, Roccabianca M, Marvaldi J, Pommier G. des-(1-3)-IGF-I, an insulin-like growth factor analog used to mimic a potential IGF-II autocrine loop, promotes the differentiation of human colon-carcinoma cells. Int J Cancer 1992;52:910 – 7.

9. Ma J, Pollak MN, Giovannucci E, et al. Prospective study of colorectal cancer risk in men and plasma levels of insulin-like growth factor (IGF)-I and IGF-binding protein-3. J Natl Cancer Inst 1999;91:620 – 5.

10. Harper J, Burns JL, Foulstone EJ, Pignatelli M, Zaina S, Hassan AB. Soluble IGF2 receptor rescues Apc(Min/+) intestinal adenoma progression induced by Igf2 loss of imprinting. Cancer Res 2006;66:1940 – 8.

11. Foulstone E, Prince S, Zaccheo O, et al. Insulin-like growth factor ligands, receptors, and binding proteins in cancer. J Pathol 2005;205: 145 – 53.

12. Baserga R. The insulin-like growth factor I receptor: a key to tumor growth? Cancer Res 1995;55:249 – 52.

13. Sell C, Rubini M, Rubin R, Liu JP, Efstratiadis A, Baserga R. Simian virus 40 large tumor antigen is unable to transform mouse embryonic fibroblasts lacking type 1 insulin-like growth factor receptor. Proc Natl Acad Sci U S A 1993;90:11217 – 21.

14. Liu JP, Baker J, Perkins AS, Robertson EJ, Efstratiadis A. Mice carrying null mutations of the genes encoding insulin-like growth factor I (Igf-1) and type 1 IGF receptor (Igf1r). Cell 1993;75:59 – 72.

15. Lahm H, Suardet L, Laurent PL, et al. Growth regulation and co-stimulation of human colorectal cancer cell lines by insulin-like growth factor I, II and transforming growth factor α. Br J Cancer 1992;65:341 – 6.

16. Thompson MA, Cox AJ, Whitehead RH, Jonas HA. Autocrine regulation of human tumor cell proliferation by insulin-like growth factor II: an *in-vitro* model. Endocrinology 1990;126:3033 – 42.

17. Chen SC, Chou CK, Wong FH, Chang CM, Hu CP. Overexpression of epidermal growth factor and insulin-like growth factor-I receptors and autocrine stimulation in human esophageal carcinoma cells. Cancer Res 1991;51:1898 – 903.

18. Imsumran A, Adachi Y, Yamamoto H, et al. Insulin-like growth factor-I receptor as a marker for prognosis and a therapeutic target in human esophageal squamous cell carcinoma. Carcinogenesis 2007;28:947 – 56.

19. Caro JF, Poulos J, Ittoop O, Pories WJ, Flickinger EG, Sinha MK. Insulin-like growth factor I binding in hepatocytes from human liver, human hepatoma, and normal, regenerating, and fetal rat liver. J Clin Invest 1988;81:976 – 81.

20. Verspohl EJ, Maddux BA, Goldfine ID. Insulin and insulin-like growth factor I regulate the same biological functions in HEP-G2 cells via their own specific receptors. J Clin Endocrinol Metab 1988;67: 169 – 74.

21. Kim SO, Park JG, Lee YI. Increased expression of the insulin-like growth factor I (IGF-I) receptor gene in hepatocellular carcinoma cell lines: implications of IGF-I receptor gene activation by hepatitis B virus X gene product. Cancer Res 1996;56:3831 – 6.

22. Bergmann U, Funatomi H, Yokoyama M, Beger HG, Korc M. Insulin-like growth factor I overexpression in human pancreatic cancer: evidence for autocrine and paracrine roles. Cancer Res 1995;55:2007 – 11.

23. Simmons JG, Pucilowska JB, Lund PK. Autocrine and paracrine actions of intestinal fibroblast-derived insulin-like growth factors. Am J Physiol 1999;276:G817 – 27.

24. Freier S, Weiss O, Eran M, et al. Expression of the insulin-like growth factors and their receptors in adenocarcinoma of the colon. Gut 1999;44: 704 – 8.

25. Ajisaka H, Fushida S, Yonemura Y, Miwa K. Expression of insulin-like growth factor-2, c-MET, matrix metalloproteinase-7 and MUC-1 in primary lesions and lymph node metastatic lesions of gastric cancer. Hepatogastroenterology 2001;48:1788 – 92.

26. Levitt RJ, Pollak M. Insulin-like growth factor-I antagonizes the antiproliferative effects of cyclooxygenase-2 inhibitors on BxPC-3 pancreatic cancer cells. Cancer Res 2002;62:7372 – 6.

27. Pandini G, Frasca F, Mineo R, Sciacca L, Vigneri R, Belfiore A. Insulin/insulin-like growth factor I hybrid receptors have different biological characteristics depending on the insulin receptor isoform involved. J Biol Chem 2002;277:39684 – 95.

28. Frasca F, Pandini G, Scalia P, et al. Insulin receptor isoform A, a newly recognized, high-affinity insulin-like growth factor II receptor in fetal and cancer cells. Mol Cell Biol 1999;19:3278 – 88.

29. Schoen RE, Weissfeld JL, Kuller LH, et al. Insulin-like growth factor-I and insulin are associated with the presence and advancement of adenomatous polyps. Gastroenterology 2005;129:464 – 75.

30. Burtrum D, Zhu Z, Lu D, et al. A fully human monoclonal antibody to the insulin-like growth factor I receptor blocks ligand-dependent signaling and inhibits human tumor growth *in vivo*. Cancer Res 2003; 63:8912 – 21.

31. Cohen BD, Baker DA, Soderstrom C, et al. Combination therapy enhances the inhibition of tumor growth with the fully human anti-type 1 insulin-like growth factor receptor monoclonal antibody CP-751,871. Clin Cancer Res 2005;11:2063 – 73.

32. Wang Y, Hailey J, Williams D, et al. Inhibition of insulin-like growth factor-I receptor (IGF-IR) signaling and tumor cell growth by a fully human neutralizing anti-IGF-IR antibody. Mol Cancer Ther 2005;4:1214 – 21.

33. Mitsiades CS, Mitsiades NS, McMullan CJ, et al. Inhibition of the insulin-like growth factor receptor-1 tyrosine kinase activity as a therapeutic strategy for multiple myeloma, other hematologic malignancies, and solid tumors. Cancer Cell 2004;5:221 – 30.

34. Wittman M, Carboni J, Attar R, et al. Discovery of a (1H-benzoimidazol-2-yl)-1H-pyridin-2-one (BMS-536924) inhibitor of insulin-like growth factor I receptor kinase with *in vivo* antitumor activity. J Med Chem 2005;48:5639 – 43.

35. Haluska P, Carboni JM, Loegering DA, et al. *In vitro* and *in vivo* antitumor effects of the dual insulin-like growth factor-I/insulin receptor inhibitor, BMS-554417. Cancer Res 2006;66:362 – 71.

36. Adachi Y, Lee CT, Coffee K, et al. Effects of genetic blockade of the insulin-like growth factor receptor in human colon cancer cell lines. Gastroenterology 2002;123:1191 – 204.

37. Min Y, Adachi Y, Yamamoto H, et al. Genetic blockade of the insulin-like growth factor-I receptor: a promising strategy for human pancreatic cancer. Cancer Res 2003;63:6432 – 41.

38. Min Y, Adachi Y, Yamamoto H, et al. Insulin-like growth factor I receptor blockade enhances chemotherapy and radiation responses and inhibits tumour growth in human gastric cancer xenografts. Gut 2005;54: 591 – 600.

39. Garcia-Echeverria C, Pearson MA, Marti A, et al. *In vivo* antitumor activity of NVP-AEW541-A novel, potent, and selective inhibitor of the IGF-IR kinase. Cancer Cell 2004;5:231 – 9.

40. Hopfner M, Baradari V, Huether A, Schofl C, Scherubl H. The insulin-like growth factor receptor 1 is a promising target for novel treatment approaches in neuroendocrine gastrointestinal tumours. Endocr Relat Cancer 2006;13:135 – 49.

41. Hopfner M, Huether A, Sutter AP, Baradari V, Schuppan D, Scherubl H. Blockade of IGF-1 receptor tyrosine kinase has antineoplastic effects in hepatocellular carcinoma cells. Biochem Pharmacol 2006;71:1435 – 48.

42. Lahm H, Amstad P, Wyniger J, et al. Blockade of the insulin-like growth-factor-I receptor inhibits growth of human colorectal cancer cells: evidence of a functional IGF-II-mediated autocrine loop. Int J Cancer 1994; 58:452 – 9.

43. Barbier M, Attoub S, Calvez R, et al. Tumour biology. Weakening link to colorectal cancer? Nature 2001;413:796.

44. Adams TE, Epa VC, Garrett TP, Ward CW. Structure and function of the type 1 insulin-like growth factor receptor. Cell Mol Life Sci 2000;57: 1050 – 93.

45. Warshamana-Greene GS, Litz J, Buchdunger E, Hofmann F, Garcia-Echeverria C, Krystal GW. The insulin-like growth factor-I (IGF-I) receptor kinase inhibitor NVP-ADW742, in combination with STI571, delineates a spectrum of dependence of small cell lung cancer on IGF-I and stem cell factor signaling. Mol Cancer Ther 2004;3:527 – 35.

46. Manara MC, Landuzzi L, Nanni P, et al. Preclinical *in vivo* study of new insulin-like growth factor-I receptor-specific inhibitor in Ewing's sarcoma. Clin Cancer Res 2007;13:1322 – 30.

47. Zhang H, Pelzer AM, Kiang DT, Yee D. Down-regulation of type I insulin-like growth factor receptor increases sensitivity of breast cancer cells to insulin. Cancer Res 2007;67:391 – 7.

48. Lu Y, Zi X, Zhao Y, Mascarenhas D, Pollak M. Insulin-like growth factor-I receptor signaling and resistance to trastuzumab (Herceptin). J Natl Cancer Inst 2001;93:1852 – 7.

49. Nahta R, Yuan LX, Zhang B, Kobayashi R, Esteva FJ. Insulin-like growth factor-I receptor/human epidermal growth factor receptor 2 heterodimerization contributes to trastuzumab resistance of breast cancer cells. Cancer Res 2005;65:11118 – 28.

50. Sbraccia P, D'Adamo M, Leonetti F, et al. Chronic primary hyperinsulinaemia is associated with altered insulin receptor mRNA splicing in muscle of patients with insulinoma. Diabetologia 1996;39:220 – 5.